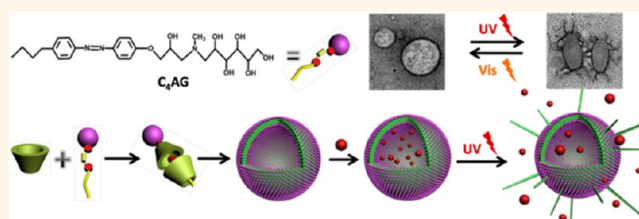


Smart Nanocarrier: Self-Assembly of Bacteria-like Vesicles with Photoswitchable Cilia

Qiang Zhao,[†] Yao Wang,[‡] Yun Yan,^{*,†} and Jianbin Huang^{*,†}

[†]Beijing National Laboratory for Molecular Sciences (BNLMS), State Key Laboratory for Structural Chemistry of Unstable and Stable Species, College of Chemistry and Molecular Engineering, Peking University, Beijing 100871, People's Republic of China; and [‡]Beijing National Laboratory for Molecular Sciences (BNLMS), Key Laboratory of Polymer Chemistry and Physics of the Ministry of Education, College of Chemistry and Molecular Engineering, Peking University, Beijing 100871, People's Republic of China

ABSTRACT Bioinspired cell deformation aids in the design of smart functional molecular self-assemblies. We report on a system of bacteria-like vesicles which release entrapped drug upon developing hairs triggered by UV irradiation, just like cilia stretching from the surface of bacteria. The formation of cilia leads to a less intact membrane, which allows release of entrapped drug. This bioinspired design created a smart nanocarrier that releases the payload via deformation rather than complete breaking.



KEYWORDS: controlled release · photoresponsive · self-assembly · vesicle · bioinspired structure · azobenzene · cyclodextrin

Smart molecular self-assemblies are attracting intense interest in the field of controlled release.¹ This usually involves the invention of smart supramolecular structures which are responsive to external stimuli such as pH,^{2–6} light,^{7–14} or chemicals.^{15–19} The load is often sealed in the inner cavity of a hollow self-assembly, such as vesicles^{20–23} and nanotubes.^{24–27} Upon exerting a stimulus, the vesicles or nanotubes are broken so that the load is released. For example, Burdick *et al.* described synthetic polymersomes which can be degraded by ultraviolet light.²⁸ Similarly, the groups of Kataoka,^{1–3} Harada,²⁹ Eisenberg,^{30,31} Lecommandoux,^{32,33} Klok,³⁴ Armes,^{35,36} and others also have done excellent work on stimuli-responsive vesicles. Generally speaking, stimuli triggered complete breaking of vesicles was employed in most designs of smart releasing systems.

In contrast to the thorough breaking of synthetic vesicles, nature usually employs a mild deformation process to express functions. As an example, blood platelets may develop many branches and irregular shapes to form a blood clot to block the wound when the tissue suffers a cut.^{37–39} Since synthetic vesicles are serving as an

excellent model to mimic the dynamic and structural features of cells, scientists have to consider: is it possible to design a vesicular system that mimics the living cells to release load with deformability rather than breaking? In this regard, so far no solution has been provided in the field of supramolecular chemistry.

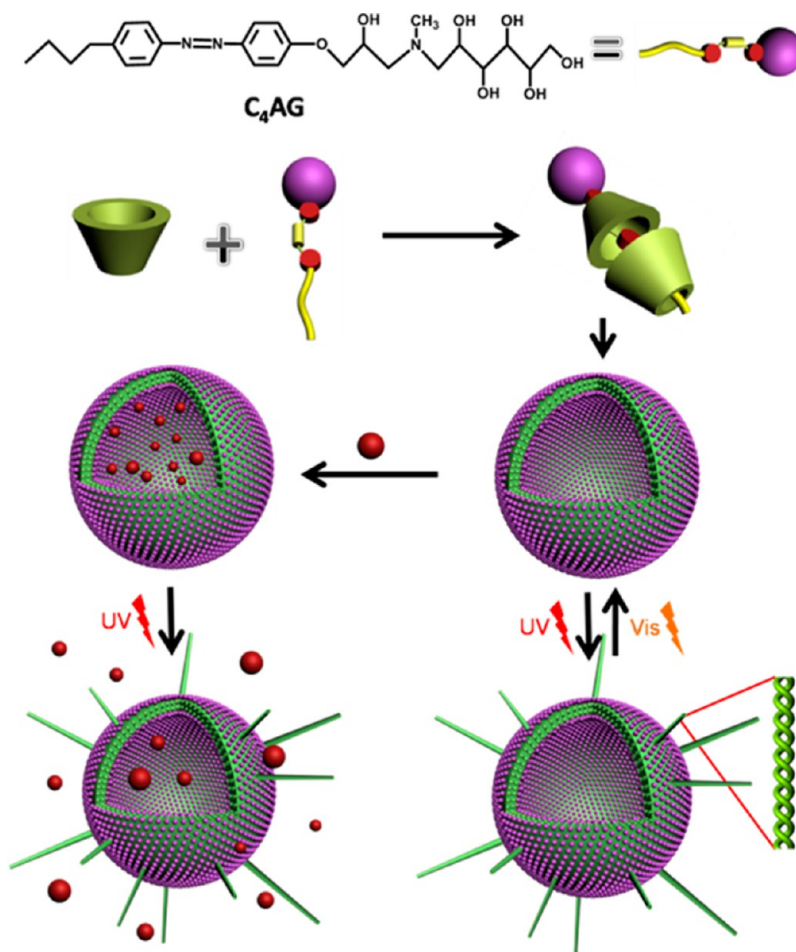
Herein we report a smart bacteria-like vesicle which may release the loaded drug as the cilia is developed under UV irradiation. The vesicles were prepared through the self-assembly of the channel-type host-guest inclusion complex of the amphiphilic [4-butyl-4'-(oxy-2,3-epoxypropyl)azobenzene] (C₄AG) and β -cyclodextrin (β -CD) in water. We have reported in our previous work that β -CD may form channel type dimers when it complexed with surfactants at a 2:1 molar ratio.⁴⁰ This surfactant@ 2β -CD complex may self-assemble into various nanostructures.^{25,41,42} In the present C₄AG@ 2β -CD vesicular systems, many hairs may develop from the surface of the vesicle upon UV irradiation, just like cilia of bacteria. Concomitantly, this triggers the release of the loaded drug. Furthermore, in analogy with living cells, the hairy vesicle is able to withdraw their hairs when exposed to visible

* Address correspondence to yunyan@pku.edu.cn, jbh Huang@pku.edu.cn.

Received for review July 30, 2014 and accepted November 2, 2014.

Published online November 02, 2014
10.1021/nn5042366

© 2014 American Chemical Society



Scheme 1. Schematic demonstration of photo-triggered release from the bacteria-like $C_4AG@2\beta$ -CD vesicles.

light. This process is reversible and repeatable with alternative UV/vis light irradiation. In this way, we are able to achieve a bacteria-like vesicle with photogated on and off cilia which govern the closure of vesicle membrane. Cell-culture experiments suggest that this bacteria-like $C_4AG@2\beta$ -CD vesicle is a nontoxic carrier that shows excellent *in vitro* photoswitchable drug releasing. We expect that this bacteria-like vesicle opens a new vista in the design of biomimetic vesicles and smart controlled releasing systems and may also aid in the understanding of the mechanism of cell deformation.

RESULTS AND DISCUSSION

The amphiphilic C_4AG which contains a sugar-like polar head and butyl azobenzene portion (Scheme 1) was synthesized in our laboratory.⁴³ We have reported that C_4AG molecules could self-assemble into a double helix (Figure 1a) in water. In this work, β -CD was added to the aqueous system of C_4AG which contains a double helix. It was noticed that the turbidity decreases at the beginning and then increases sharply with a further increase of the amount of β -CD (Figure 1b). This suggests that the host–guest interaction between C_4AG and β -CD has induced the self-assembly

transition. Transmission electron microscopy (TEM) measurements revealed the formation of vesicles after addition of β -CD (Figure 1c and Figure S1, Supporting Information). It is noted that the vesicles start to occur at the ratio of C_4AG/β -CD = 1:2 where some helices still exist (Figure 1d). Complete vesicle formation is found at C_4AG/β -CD beyond 1:3. At a lower C_4AG/β -CD ratio of 1:2, such as 1:0.5 and 1:1, vesicles can hardly be observed (Figure S2, Supporting Information). In addition, there are always some fragments accompanied by the vesicle formation, and dynamic light scattering (DLS) always gives a very broad peak which makes the sizing analysis with DLS less informative (Figure S3, Supporting Information).

The formation of inclusion complexes between C_4AG/β -CD was confirmed by UV–vis and 1H NMR. Parts a and b of Figure 2 show that the π – π^* absorption of the *trans*-azobenzene at 346 nm shifts toward red as β -CD is added. The absorption peak at 356 nm reaches a maximum at a molar ratio of C_4AG/β -CD = 1:2. Meanwhile, parts c and d of Figure 2 reveal that the chemical shifts of protons in the azobenzene group of C_4AG have moved to a higher field upon addition of β -CD. The chemical shifts for the H3 and H5 protons of β -CD are the smallest at a ratio of 1:2, which is in

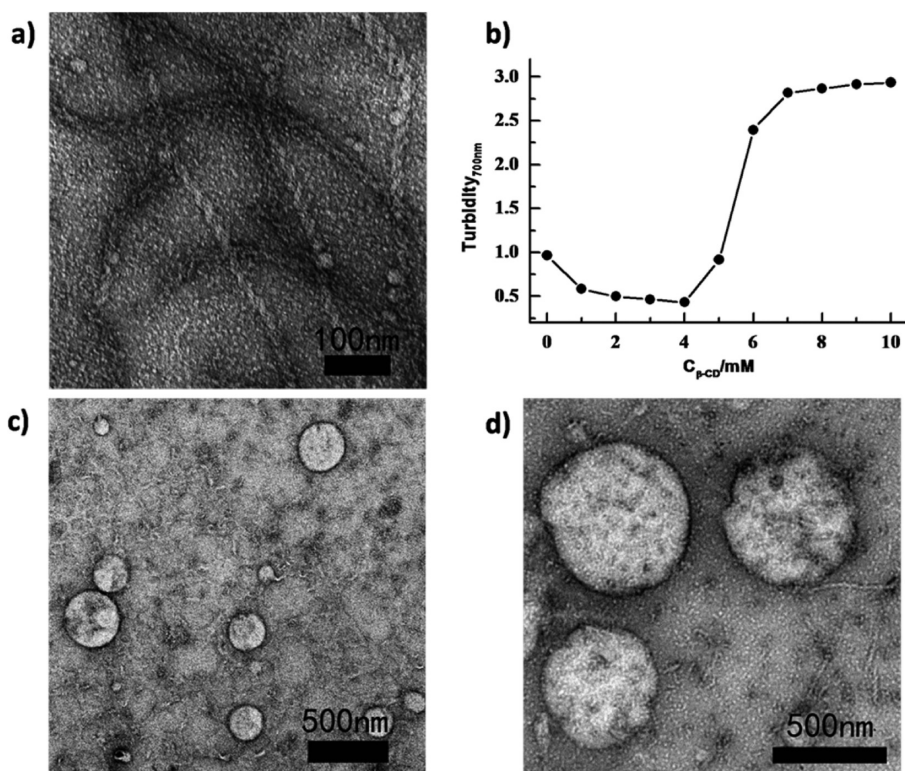


Figure 1. (a) TEM images of double helix formed in the aqueous system of C_4AG . (b) Change of turbidity in the C_4AG aqueous system upon addition of β -CD (at 700 nm, 25 °C). (c, d) are the TEM images of vesicles formed at $C_{C_4AG}/C_{\beta\text{-CD}} = 1:3$ and $1:2$, respectively. In all measurements, the concentration of C_4AG is 2 mM.

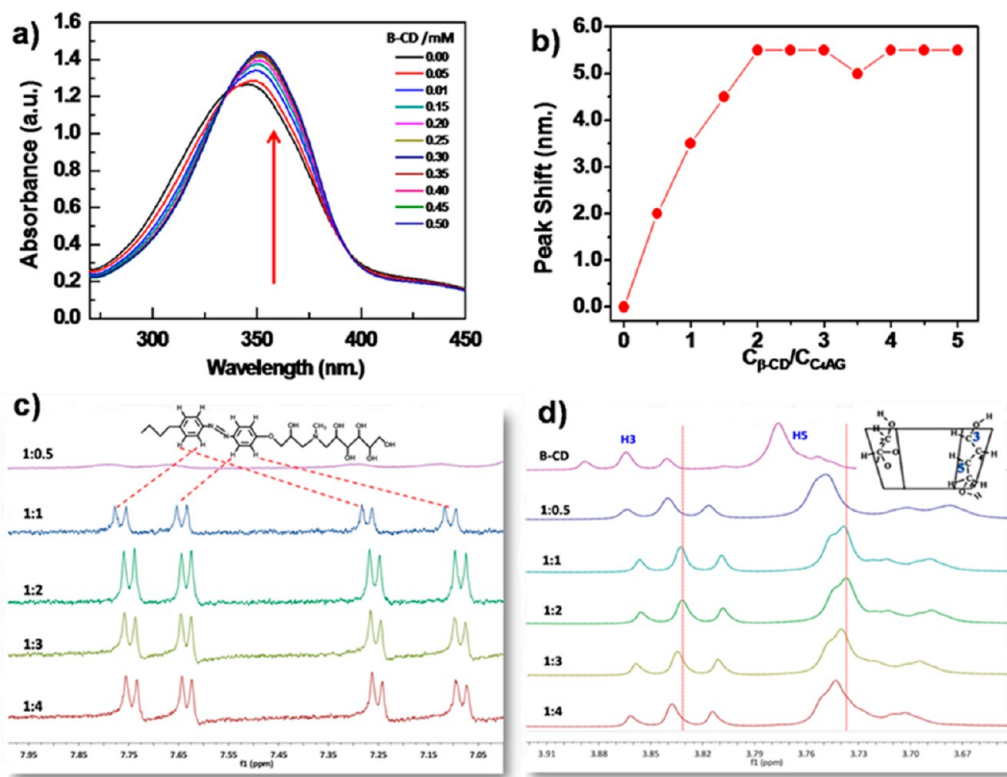


Figure 2. (a) UV-vis spectra of 0.1 mM C_4AG in the presence of various concentrations of β -CD (0–0.5 mM); (b) peak shift of the maximum absorption at 356 nm with the $C_{\beta\text{-CD}}/C_{C_4AG}$ ratios; (c) ^1H NMR spectra of H of azobenzene group at the C_4AG/β -CD molar ratios of 1:0.5, 1:1, 1:2, 1:3, and 1:4; (d) ^1H NMR spectra of the H3 and H5 of β -CD at the C_4AG/β -CD molar ratios of 1:0 (β -CD), 1:0.5, 1:1, 1:2, 1:3 and 1:4. The solvent was D_2O .

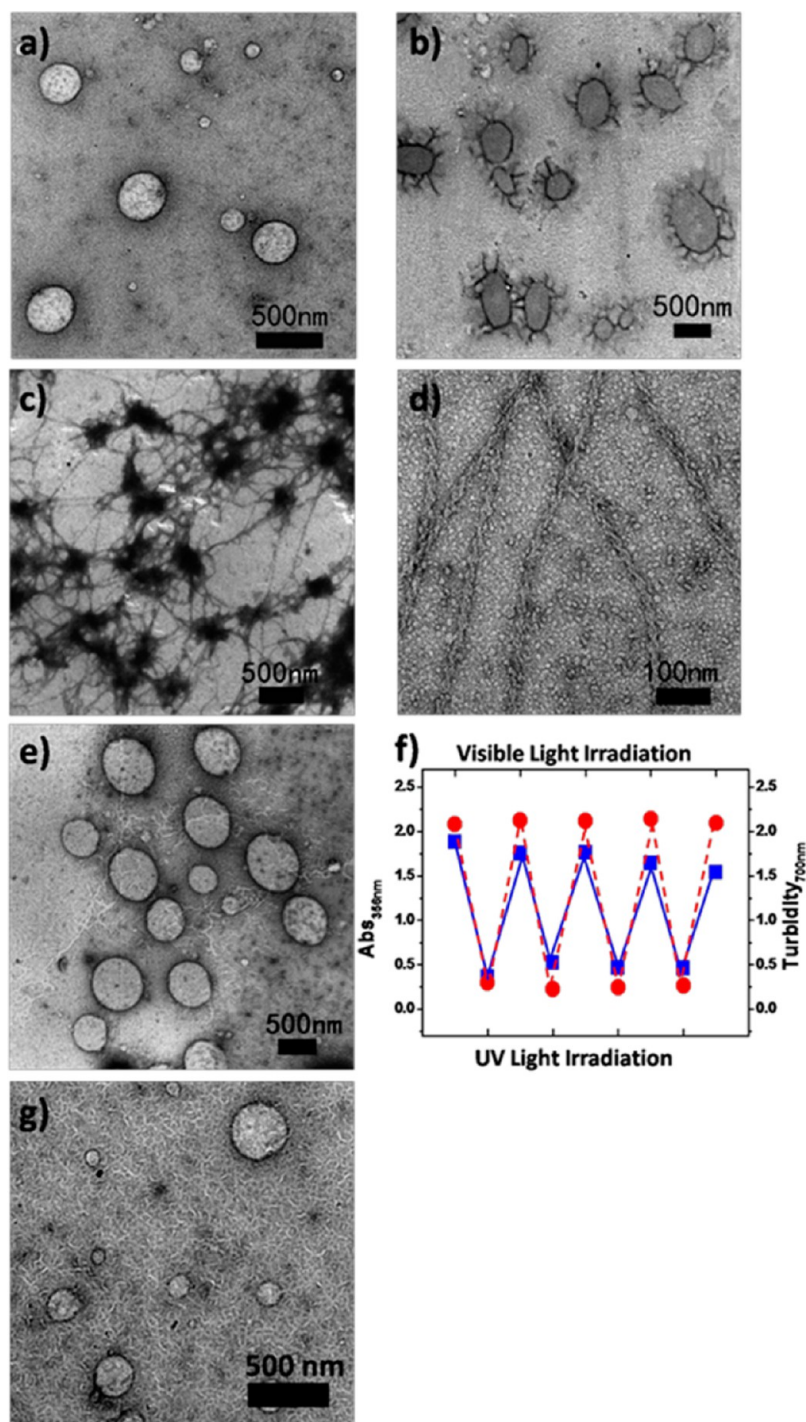


Figure 3. TEM images of (a) $C_4AG@2\beta$ -CD vesicles and the vesicles exposed to UV light for (b) 10 min, (c) 1 h, and (d) 6 h. (e) Vesicles are observed again after the ciliated vesicles in (b) are exposed to visible light for 6 h. (f) Repeated absorbance (blue line, at 356 nm) and turbidity (red dot, at 700 nm) of $C_4AG@2\beta$ -CD. The concentrations for these two measurements are 0.1 mM/0.2 mM and 2 mM/6 mM C_4AG/β -CD, respectively. (g) TEM image of the $C_4AG@2\beta$ -CD vesicles after four cycles of UV and visible light irradiation. It can be observed that that the size of the vesicles is almost the same as that in (a).

agreement with the position where the maximum UV absorption occurs, indicating two β -CDs have been connected by one C_4AG to form channel-type dimers. This complex is recorded as $C_4AG@2\beta$ -CD. Obviously, the $C_4AG@2\beta$ -CD supramolecular complex has acted as the basic building block which self-assembles into a vesicle. Since all of the hydrophobic portions of C_4AG

are buried in the cavity of β -CD, these vesicles have to be driven by hydrogen bonding, which is similar to the vesicles in $SDS@2\beta$ -CD supramolecular systems.⁴²

The $C_4AG@2\beta$ -CD vesicles are able to respond to UV light. Figure 3 shows the TEM observation of the vesicles over time. Without UV irradiation, the vesicles were spherical in solution (Figure 3a). After 10 min of

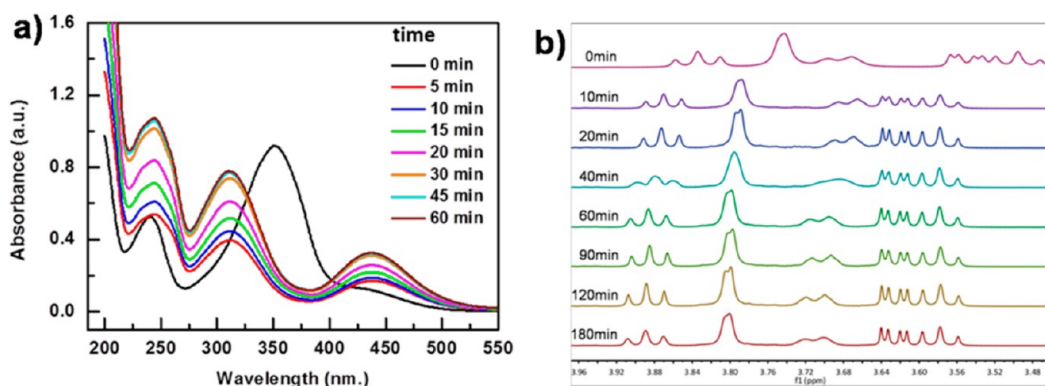


Figure 4. (a) Time-dependent UV–vis spectrum of C₄AG@2β-CD (0.1 mM/0.2 mM) aqueous solution and (b) ¹H NMR spectra of H3 and H5 in C₄AG@2β-CD (1 mM/2 mM) upon UV irradiation.

UV irradiation, some hairs started to “grow” on the surface of the vesicles (Figure 3b and Figure S4, Supporting Information), just like cilia of bacteria. The cilia may grow much longer with time, accompanied by the collapse of vesicles (Figure 3c). Figure 3d demonstrates that after 12 h of irradiation, no vesicles could survive and only cilia are present. The zoomed-in image indicates that the cilia have the features of a helix. This means that the development of cilia is the intermediate stage of the transformation from vesicles to helices. However, the cilia were not the same helix as that formed with free C₄AG. In the C₄AG@2β-CD system, one C₄AG could be included in two cyclodextrins (Figure 2c,d). The one covering the azobenzene moiety will leave the C₄AG under UV irradiation; the other, which locates on the alkyl section, keeps the inclusion state. As a result, after a long UV irradiation time, all of the *trans*-azobenzene was reverted to the *cis*-form, but there was still one cyclodextrin complexing with the alkyl chain of the C₄AG, which was confirmed by ¹H NMR measurement (Figure S5, Supporting Information). Hence, it was not the *cis*-C₄AG but the *cis*-C₄AG@β-CD form in the helix after UV irradiation. The reason for the formation of helix from *cis*-C₄AG@β-CD is probably due to the hydrogen bonding and steric effect.

The transitions in the C₄AG@2β-CD system were reversible. Figure 3e reveals that after the 12 h irradiated sample was subjected to visible light for 6 h, vesicles were observed again. Meanwhile, the change in microstructure, UV absorbance, and turbidity could lead to a reversion to the original state after the sample was alternatively subjected to UV and visible light irradiation. The blue line in Figure 3f demonstrates that the intensity of absorbance at 356 nm oscillates between 1.6 and 0.5, which indicates the reversible transition between *trans*- and *cis*-azobenzene group. In analogy, the turbidity at 700 nm also exhibits similar oscillations which indicate an alternative change between vesicles and helix (Figure 3f, red dot). TEM observations (Figure 3g) suggest that vesicles can still be observed after four such cycles. It is worth noting

that even the size of these vesicles is not changed obviously compared with that in Figure 3a, suggesting this self-assembling behavior is the genetic property of this system.

The formation of bacteria-like vesicles in the C₄AG@2β-CD system upon UV irradiation can be attributed to the slow detaching dynamics of *cis*-C₄AG from β-CD. Although the UV–vis measurements revealed that the *trans*-C₄AG disappeared within 5 min, the absorbance of *cis*-isomer was observed to amount to the maximum within 1 h (Figure 4a). Meanwhile, ¹H NMR results indicated it tooks more than 1 h for the chemical shifts of the H3 and H5 protons in β-CD to reach equilibrium states (Figure 4b). This means that detaching of β-CD from the *cis*-azobenzene group is time-consuming. The slow process is probably due to the remaining interactions between C₄AG and β-CD when the C₄AG@2β-CD supramolecular tile was disassembled upon UV irradiation. These interactions may include the inclusion of the butyl tail of C₄AG into the cavity of β-CD or the hydrogen bonding between the headgroup of C₄AG and β-CD. This on the one hand retains the C₄AG on the surface of the original vesicles and on the other hand slows down the self-assembly of C₄AG into the double helix. These two criteria finally produce the scenario of “cilia” on the surface of the vesicles before they completely transform into double helices.

The transformation between vesicles and helices indicates the development of cilia is at the cost of membrane-forming molecules. This means that with the development of the cilia, the intactness of the vesicles should be weakened. Therefore, the bacteria-like vesicles with cilia may release any drug that is preloaded. It is indeed the case. TEM measurements revealed that the vesicular structure remained intact after doxorubicin hydrochloride (DOX), which is an anti-cancer drug, was encapsulated in the C₄AG@2β-CD vesicles (Figure 5a and 5b). AFM measurement showed that the drug-loaded vesicle was about 50 nm in height, but the hollow one was just about 10 nm in height (Figure 5,d). Obviously, the vesicles loaded with

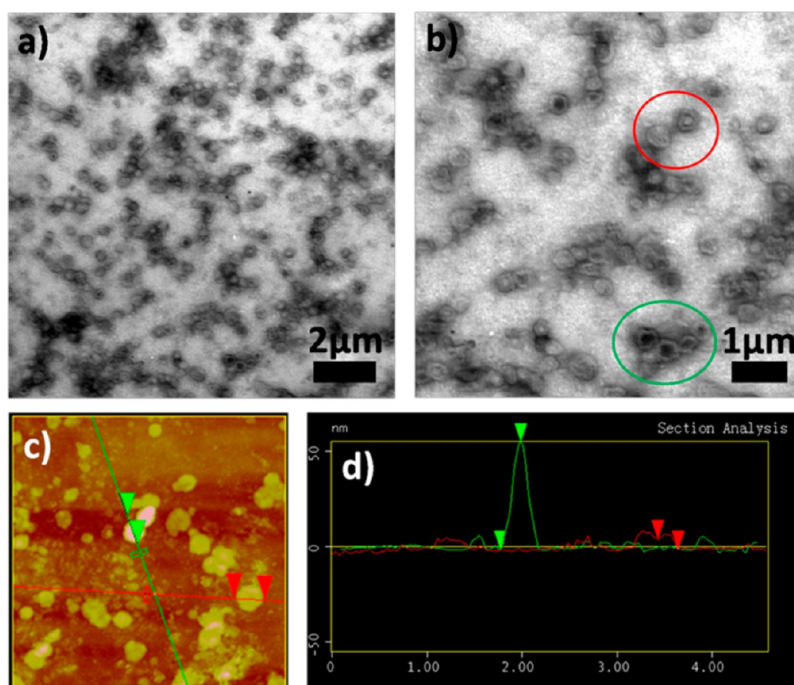


Figure 5. (a, b) TEM images of vesicles (in the green circle) loaded with DOX. The red circle indicates the presence of some empty vesicles without DOX inside. (c, d) AFM images and height profiles of the vesicles with (green) and without drug loaded (red), respectively.

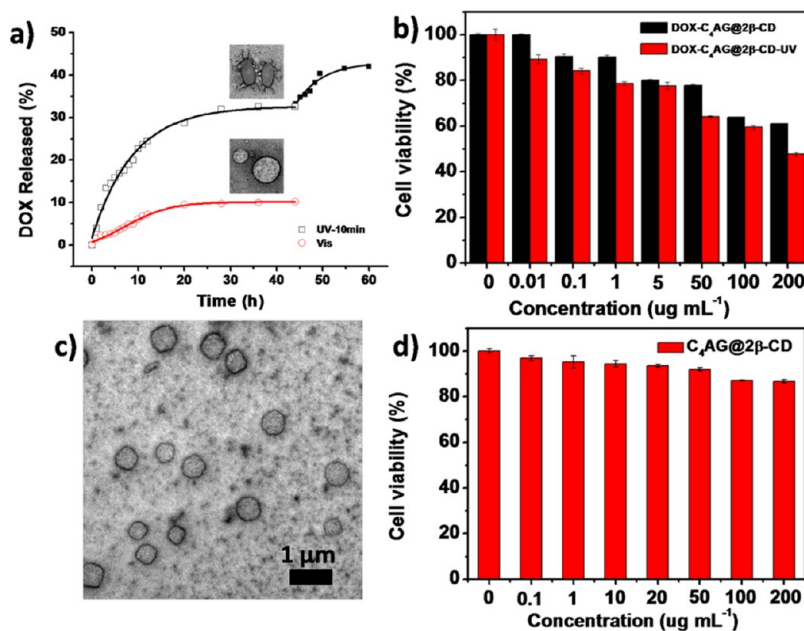


Figure 6. (a) Drug-release profiles and (b) cytotoxicity of DOX-loaded vesicles under visible light (black) and ultraviolet light for 10 min (red) in PBS at pH 7.4 and 37 °C *in vitro* measured with HeLa cells. (c) TEM image of $C_4AG@2\beta$ -CD vesicles in DMEM solution at molar ratios of C_4AG/β -CD = 1:3. (d) Cytotoxicity of $C_4AG@2\beta$ -CD vesicles to HeLa cells after 48 h. Data were presented as the mean \pm standard deviation ($n = 3$).

drug are more robust against collapse. Encapsulation efficiency measurements suggested that about 12.6% (w/w) of DOX was encapsulated in the $C_4AG@2\beta$ -CD vesicles.

The drug-loaded vesicles could also be broken under UV irradiation. Figure 6a shows that about 32.5% entrapped DOX is released upon UV irradiation for 10 min.

Further release can be achieved upon exerting another interval of UV stimulus. The curve across the solid squares at the end of the releasing curve in Figure 6a shows that about extra 10% of DOX was released when the releasing system was subjected to another 10 min UV irradiation. This suggests that the release can be controlled step by step. This is a fairly interesting result

since it makes the control over the quantity of release possible. Although at present only about 60%, instead of 100%, of the entrapped DOX can be released at most due to the possible interactions between DOX and the vesicle components (which is actually a common problem in controlled releasing systems⁴⁴), we expect that it is still an exciting step toward the complete “control” of drug release in the future.

The release of DOX resulted in the decrease of the viability of HeLa and C6 glioma cells. Figure 6b shows that the viability of the HeLa cells after 10 min of UV irradiation is obviously lower than that before irradiation. This tendency became much clearer with increasing concentrations. A similar tendency was observed for C6 glioma cells as well (Figure S6, Supporting Information). This tells that the vesicle membrane is more intact at high concentrations, and the development of cilia has indeed lowered the intactness of the vesicles. This is analogue to the functional changes caused by the morphology change of cells in living systems. It should be mentioned that the C₄AG@2β-CD could still form stable vesicles in DMEM solution which is the cell culture (Figure 6c), although the vesicular size became larger due to the shielding effect of the salt in DMEM. Since cytotoxicity of C₄AG@2β-CD vesicles is

negligible to cells (Figure 6d), they are expected to be potentially used as a biocompatible drug carrier that has *in vitro* applications.

CONCLUSION

In conclusion (Scheme 1), we have constructed a bacteria-like vesicular system based on the slow vesicle to helix transition process of the self-assembly of channel type β-CD dimers induced by a photoresponsive azobenzene amphiphile C₄AG. UV irradiation breaks the channel type C₄AG@2β-CD supramolecular building block, yet the remaining interactions, including the hydrogen bonding between β-CD and the head of C₄AG, or the host–guest interaction between the butyl group of C₄AG and the cavity of β-CD, slow down the leave of both components from the vesicles. Therefore, they may have time to self-assemble into helices on the surface of vesicles, resembling cilia of bacteria. The wall for vesicles with cilia becomes less intact which allows leaking of the entrapped drug or other materials. Since deformation of cells is universal in biological process, we expect the mode of releasing describe in this work may inspire smart design of biomimetic vesicles and help to understand the mechanism of cell deformation.

EXPERIMENTAL SECTION

Materials. The C₄AG was synthesized according to our previous work.⁴³ β-CD was purchased from Sinopharm Chemical Reagent Co. with a water content of 14%. D₂O (99.9%) was purchased from Cambridge Isotope Laboratories, Inc. Aqueous solutions were prepared using Milli-Q water of 18 MΩ. Sulforhodamine B (SRB) was purchased from Sigma-Aldrich (St. Louis, MO). Other reagents were from Beijing Chemical Reagents (Beijing, China). All reagents were used as received, and the solvents were purified according to the previous general procedures.

Spectra Measurements. UV–vis absorbance measurements were carried out on the Pgeneral TU-1810 UV–vis spectrophotometer. Absorbance measurements and turbidity measurements were carried out at 356 and 700 nm, respectively. All of the spectral measurements were conducted at room temperature (RT).

¹H Nuclear Magnetic Resonance (¹H NMR). The ¹H NMR experiments were performed on a Bruker ARX 400 MHz spectrometer with D₂O as solvent.

Transmission Electron Micrograph (TEM). Samples were observed by a JEOL JEM 100CX, 80 kV, and JEM-2100, 200 kV. Drops of samples were put onto 230 mesh copper grids coated with Formvar film. As described previously,⁴⁵ excess water was removed by filter paper, and the samples were stained and then allowed to dry in ambient air at rt before TEM observation.

Doxorubicin Loading. Doxorubicin hydrochloride (DOX) was loaded using an equilibrium dialysis method as described previously.⁴⁶ DOX hydrochloride (1 mg) was mixed with 1 mg of C₄AG@2β-CD, and the solution was heated at 50 °C for 1 h. Then the solution was placed in dark for 72 h at 25 °C. The solution was further transferred to a dialysis bag (MWCO = 3500) against water in the dark for 72 h to remove free DOX, C₄AG, and β-CD molecules. The encapsulation percentage of DOX was determined by UV–vis scanning spectrophotometry at 480 nm in water. DOX-loaded vesicles were dissolved in water and analyzed with a UV–vis scanning spectrophotometer. The calibration curve was acquired with different DOX concentrations.

Drug loading content and drug loading efficiency were calculated according to the following equations:

$$\text{drug loading content} = (\text{weight of loaded drug} / \text{weight of vesicles}) \times 100\%$$

$$\text{drug loading efficiency} = (\text{weight of loaded drug} / \text{weight of feeding drug}) \times 100\%$$

The DOX loading amount was 12.6%.

DOX Release from C₄AG@2β-CD Vesicles *in Vitro*. Dispersed DOX-loaded vesicles (5 mg mL⁻¹, ~C₄AG = 2 mM) were added to a dialysis membrane bag (MWCO = 3500), which was then incubated in 80 mL phosphate buffer saline (PBS) at pH 7.4 at 37 °C in a water bath with a shaking rate at 80 rpm. At predetermined frequencies, 3 mL of incubated solution was taken out, and 3 mL of fresh PBS was added to refill the incubation solution to 80 mL. DOX-releasing profiles were determined by measuring the UV–vis absorbance of the solutions at 480 nm. The ultraviolet-triggered DOX release measurements were conducted in the same manner as described above, but the DOX-loaded vesicles were subjected to UV irradiation for 10 min and 12 h, respectively, before dialysis. Drug release efficiency was calculated according to the following equation:

$$\text{drug release efficiency} = (\text{weight of release drug} / \text{weight of loaded drug}) \times 100\%$$

Cell Culture. In this study, HeLa and murine C6 glioma cell lines were used. The HeLa and murine C6 glioma cells (Institute of Material Medical, Chinese Academy of Medical Sciences and Peking Union Medical College, Beijing, China) were routinely grown in DMEM medium supplemented by 10% heated-inactivated fetal bovine serum (FBS), 100 U mL⁻¹ of penicillin, and 100 mg mL⁻¹ of streptomycin. Cells were maintained at 37 °C with 5% CO₂.

***In Vitro* Cytotoxicity Assay.** HeLa cells or C6 cells were seeded into 96-well culture plates at a density of 5 × 10³ cells well⁻¹ and grown for 24 h. Then C₄AG@2β-CD carrier was added into

96-well culture plates. The concentration of $C_4AG@2\beta$ -CD carrier was in the range of 0–100 $\mu\text{g mL}^{-1}$. After 48 h incubation, the cell viability was measured by a microplate reader at 540 nm with the SRB staining assay. The following formula was used: survival (%) = $(A_{540\text{ nm}} \text{ for the treated cells} / A_{540\text{ nm}} \text{ for the control cells}) \times 100\%$, where the $A_{540\text{ nm}}$ was the absorbance value. Each assay was repeated six times.

Conflict of Interest: The authors declare no competing financial interest.

Supporting Information Available: TEM images of C_4AG/β -CD at different ratios. DLS result of $C_4AG@2\beta$ -CD vesicles. ^1H NMR spectra of β -CD in $C_4AG@2\beta$ -CD system. Cytotoxicity of DOX-loaded vesicles for C6 glioma cells. This material is available free of charge via the Internet at <http://pubs.acs.org>.

Acknowledgment. This work is supported by National Natural Science Foundation of China (21422302, 21173011, 21273013, 51121091), the National Basic Research Program of China (973 Program, 2013CB933800), and the Doctoral Program of Higher Education of China.

REFERENCES AND NOTES

- Bae, Y.; Kataoka, K. Intelligent Polymeric Micelles from Functional Poly(ethylene glycol)-Poly(amino acid) Block Copolymers. *Adv. Drug Delivery Rev.* **2009**, *61*, 768–784.
- Oishi, M.; Kataoka, K.; Nagasaki, Y. pH-Responsive Three-Layered PEGylated Polyplex Micelle Based on A Lactosylated ABC Triblock Copolymer as A Targetable and Endosome-Disruptive Nonviral Gene Vector. *Bioconjugate Chem.* **2006**, *17*, 677–688.
- Lee, Y.; Ishii, T.; Cabral, H.; Kim, H. J.; Seo, J.-H.; Nishiyama, N.; Oshima, H.; Osada, K.; Kataoka, K. Charge-Conversional Polyionic Complex Micelles-Efficient Nanocarriers for Protein Delivery Into Cytoplasm. *Angew. Chem., Int. Ed.* **2009**, *48*, 5309–5312.
- Bellomo, E. G.; Wyrsta, M. D.; Pakstis, L.; Pochan, D. J.; Deming, T. J. Stimuli-Responsive Polypeptide Vesicles by Conformation-Specific Assembly. *Nat. Mater.* **2004**, *3*, 244–248.
- Nowag, S.; Haag, R. pH-Responsive Micro- and Nanocarrier Systems. *Angew. Chem., Int. Ed.* **2014**, *53*, 49–51.
- Sun, Z. F.; Li, Z. Y.; He, Y. H.; Shen, R. J.; Deng, L.; Yang, M. H.; Liang, Y. Z.; Zhang, Y. Ferrocenoyl Phenylalanine: A New Strategy Toward Supramolecular Hydrogels with Multistimuli Responsive Properties. *J. Am. Chem. Soc.* **2013**, *135*, 13379–13386.
- Ferris, D. P.; Zhao, Y.-L.; Khashab, N. M.; Khatib, H. A.; Stoddart, J. F.; Zink, J. I. Light-Operated Mechanized Nanoparticles. *J. Am. Chem. Soc.* **2009**, *131*, 1686–1688.
- Samanta, A.; Stuart, M. C. A.; Ravoo, B. J. Photoresponsive Capture and Release of Lectins in Multilamellar Complexes. *J. Am. Chem. Soc.* **2012**, *134*, 19909–19914.
- Zhang, Q.; Ko, N. R.; Oh, J. K. Recent Advances in Stimuli-Responsive Degradable Block Copolymer Micelles: Synthesis and Controlled Drug Delivery Applications. *Chem. Commun.* **2012**, *48*, 7542–7552.
- Kobatake, S.; Takami, S.; Muto, H.; Ishikawa, T.; Irie, M. Rapid and Reversible Shape Changes of Molecular Crystals on Photoirradiation. *Nature* **2007**, *446*, 778–781.
- Chen, X.; Hong, L.; You, X.; Wang, Y.; Zou, G.; Su, W.; Zhang, Q. Photo-Controlled Molecular Recognition of Alpha-Cyclodextrin with Azobenzene Containing Polydiacetylene Vesicles. *Chem. Commun.* **2009**, *11*, 1356–1358.
- Zhang, J.; Shen, X. Temperature-Induced Reversible Transition between Vesicle and Supramolecular Hydrogel in The Aqueous Ionic Liquid-Beta-Cyclodextrin System. *J. Phys. Chem. B* **2013**, *117*, 1451–1457.
- Liu, Y.; Yu, C.; Jin, H.; Jiang, B.; Zhu, X.; Zhou, Y.; Lu, Z.; Yan, D. A Supramolecular Janus Hyperbranched Polymer and Its Photoresponsive Self-Assembly of Vesicles with Narrow Size Distribution. *J. Am. Chem. Soc.* **2013**, *135*, 4765–4770.
- Kauscher, U.; Samanta, A.; Ravoo, B. J. Photoresponsive Vesicle Permeability Based on Intramolecular Host-Guest Inclusion. *Org. Biomol. Chem.* **2014**, *12*, 600–606.
- Liu, R.; Zhang, Y.; Feng, P. Multiresponsive Supramolecular Nanogated Ensembles. *J. Am. Chem. Soc.* **2009**, *131*, 15128–15129.
- Sheng, L.; Li, M. J.; Zhu, S. Y.; Li, H.; Xi, G.; Li, Y. G.; Wang, Y.; Li, Q. S.; Liang, S. J.; Zhong, K.; Zhang, S. X. A. Hydrochromic Molecular Switches for Water-Jet Rewritable Paper. *Nat. Commun.* **2014**, *5*.
- Guo, D.-S.; Wang, K.; Wang, Y.-X.; Liu, Y. Cholinesterase-Responsive Supramolecular Vesicle. *J. Am. Chem. Soc.* **2012**, *134*, 10244–10250.
- Li, H. M.; Yu, S. S.; Miteva, M.; Nelson, C. E.; Werfel, T.; Giorgio, T. D.; Duvall, C. L. Matrix Metalloproteinase Responsive, Proximity-Activated Polymeric Nanoparticles for siRNA Delivery. *Adv. Funct. Mater.* **2013**, *23*, 3040–3052.
- Wang, C.; Chen, Q. S.; Wang, Z. Q.; Zhang, X. An Enzyme-Responsive Polymeric Superamphiphile. *Angew. Chem., Int. Ed.* **2010**, *49*, 8612–8615.
- Wilson, D. A.; Nolte, R. J. M.; van Hest, J. C. M. Entrapment of Metal Nanoparticles in Polymer Stomatocytes. *J. Am. Chem. Soc.* **2012**, *134*, 9894–9897.
- Anraku, Y.; Kishimura, A.; Oba, M.; Yamasaki, Y.; Kataoka, K. Spontaneous Formation of Nanosized Unilamellar Polyion Complex Vesicles with Tunable Size and Properties. *J. Am. Chem. Soc.* **2010**, *132*, 1631–1636.
- Song, J. B.; Zhou, J. J.; Duan, H. W. Self-Assembled Plasmonic Vesicles of SERS-Encoded Amphiphilic Gold Nanoparticles for Cancer Cell Targeting and Traceable Intracellular Drug Delivery. *J. Am. Chem. Soc.* **2012**, *134*, 13458–13469.
- Zhang, X.; Rehm, S.; Safont-Sempere, M. M.; Wurthner, F. Vesicular Perylene Dye Nanocapsules as Supramolecular Fluorescent pH Sensor Systems. *Nat. Chem.* **2009**, *1*, 623–629.
- Biswas, S.; Kinbara, K.; Niwa, T.; Taguchi, H.; Ishii, N.; Watanabe, S.; Miyata, K.; Kataoka, K.; Aida, T. Biomolecular Robotics for Chemomechanically Driven Guest Delivery Fuelled by Intracellular ATP. *Nat. Chem.* **2013**, *5*, 613–620.
- Jiang, L. X.; de Folter, J. W. J.; Huang, J. B.; Philipse, A. P.; Kegel, W. K.; Petukhov, A. V. Helical Colloidal Sphere Structures through Thermo-Reversible Co-Assembly with Molecular Microtubes. *Angew. Chem., Int. Ed.* **2013**, *52*, 3364–3368.
- Abidian, M. R.; Kim, D. H.; Martin, D. C. Conducting-Polymer Nanotubes for Controlled Drug Release. *Adv. Mater.* **2006**, *18*, 405–409.
- Lvov, Y. M.; Shchukin, D. G.; Mohwald, H.; Price, R. R. Halloysite Clay Nanotubes for Controlled Release of Protective Agents. *ACS Nano* **2008**, *2*, 814–820.
- Katz, J. S.; Zhong, S.; Ricart, B. G.; Pochan, D. J.; Hammer, D. A.; Burdick, J. A. Modular Synthesis of Biodegradable Diblock Copolymers for Designing Functional Polymerosomes. *J. Am. Chem. Soc.* **2010**, *132*, 3654–3655.
- Bae, Y.; Fukushima, S.; Harada, A.; Kataoka, K. Design of Environment-Sensitive Supramolecular Assemblies for Intracellular Drug Delivery: Polymeric Micelles That Are Responsive to Intracellular pH Change. *Angew. Chem., Int. Ed.* **2003**, *42*, 4640–4643.
- Mai, Y.; Eisenberg, A. Controlled Incorporation of Particles into the Central Portion of Vesicle Walls. *J. Am. Chem. Soc.* **2010**, *132*, 10078–10084.
- Yu, S.; Azzam, T.; Rouiller, I.; Eisenberg, A. "Breathing" Vesicles. *J. Am. Chem. Soc.* **2009**, *131*, 10557–10566.
- Schatz, C.; Louguet, S.; Le Meins, J. F.; Lecommandoux, S. Polysaccharide-Block-Polypeptide Copolymer Vesicles: Towards Synthetic Viral Capsids. *Angew. Chem., Int. Ed.* **2009**, *48*, 2572–2575.
- Rodriguez-Hernandez, J.; Lecommandoux, S. Reversible Inside-Out Micellization of pH-Responsive and Water-Soluble Vesicles Based on Polypeptide Diblock Copolymers. *J. Am. Chem. Soc.* **2005**, *127*, 2026–2027.
- Checot, F.; Lecommandoux, S.; Gnanou, Y.; Klok, H. A. Water-Soluble Stimuli-Responsive Vesicles from Peptide-Based Diblock Copolymers. *Angew. Chem., Int. Ed.* **2002**, *41*, 1339–1343.
- Fielding, L. A.; Lane, J. A.; Derry, M. J.; Mykhaylyk, O. O.; Armes, S. P. Thermo-Responsive Diblock Copolymer Worm

- Gels in Non-Polar Solvents. *J. Am. Chem. Soc.* **2014**, *136*, 5790–5798.
36. Ladmiraal, V.; Semsarilar, M.; Canton, I.; Armes, S. P. Polymerization-Induced Self-Assembly of Galactose-Functionalized Biocompatible Diblock Copolymers for Intracellular Delivery. *J. Am. Chem. Soc.* **2013**, *135*, 13574–13581.
 37. Hollopeter, G.; Jantzen, H. M.; Vincent, D.; Li, G.; England, L.; Ramakrishnan, V.; Yang, R. B.; Nurden, P.; Nurden, A.; Julius, D.; Conley, P. B. Identification of the Platelet ADP Receptor Targeted by Antithrombotic Drugs. *Nature* **2001**, *409*, 202–207.
 38. Born, G. V. R. Aggregation of Blood Platelets by Adenosine Diphosphate and Reversal. *Nature* **1962**, *194*, 927–929.
 39. Abo, T.; Balch, C. M. A Differentiation Antigen of Human NK-Cells Identified By A Monoclonal-Antibody (HNK-1). *J. Immunol.* **1981**, *127*, 1024–1029.
 40. Jiang, L. X.; Peng, Y.; Yan, Y.; Huang, J. B. Aqueous Self-Assembly of SDS@2 Beta-CD Complexes: Lamellae and Vesicles. *Soft Matter* **2011**, *7*, 1726–1731.
 41. Jiang, L. X.; Peng, Y.; Yan, Y.; Deng, M. L.; Wang, Y. L.; Huang, J. B. "Annular Ring" Microtubes Formed by SDS@2Beta-CD Complexes in Aqueous Solution. *Soft Matter* **2010**, *6*, 1731–1736.
 42. Zhou, C. C.; Cheng, X. H.; Yan, Y.; Wang, J. D.; Huang, J. B. Reversible Transition between SDS@2Beta-CD Microtubes and Vesicles Triggered by Temperature. *Langmuir* **2014**, *30*, 3381–3386.
 43. Lin, Y. Y.; Wang, A. D.; Qiao, Y.; Gao, C.; Drechsler, M.; Ye, J. P.; Yan, Y.; Huang, J. B. Rationally Designed Helical Nanofibers via Multiple Non-Covalent Interactions: Fabrication and Modulation. *Soft Matter* **2010**, *6*, 2031–2036.
 44. Xu, J. T.; Fu, Q.; Ren, J. M.; Bryant, G.; Qiao, G. G. Novel Drug Carriers: from Grafted Polymers to Cross-Linked Vesicles. *Chem. Commun.* **2013**, *49*, 33–35.
 45. Lin, Y.; Qiao, Y.; Gao, C.; Tang, P.; Liu, Y.; Li, Z.; Yan, Y.; Huang, J. Tunable One-Dimensional Helical Nanostructures: From Supramolecular Self-Assemblies to Silica Nanomaterials. *Chem. Mater.* **2010**, *22*, 6711–6717.
 46. Chen, J.; Qiu, X.; Ouyang, J.; Kong, J.; Zhong, W.; Xing, M. M. Q. pH and Reduction Dual-Sensitive Copolymeric Micelles for Intracellular Doxorubicin Delivery. *Biomacromolecules* **2011**, *12*, 3601–3611.